Laser-induced fluorescence characterization of a multidipole filament plasma

M. J. Goeckner,[a] J. Goree,[b] and T. E. Sheridan[c]
Department of Physics and Astronomy, The University of Iowa, Iowa City, Iowa 52242

(Received 5 September 1990; accepted 11 June 1991)

A multidipole filament discharge was characterized using sub-Doppler laser-induced fluorescence (LIF). The ion temperature was found to be $T_i = 0.028 \pm 0.007$ eV, measured in the center of an argon discharge. This stands in contrast to the much higher ion temperatures, $0.2 < T_i < 0.5$ eV, reported by researchers using gridded electrostatic energy analyzers. The discrepancy is attributed to the energy resolution of the detectors, with the LIF providing more accurate measurements. In another result, the metastable excited-state ion density was found to scale linearly with the electron density and the discharge current under most conditions. This experiment also demonstrates that LIF can be used for basic plasma physics research in multidipole discharges.

I. INTRODUCTION

Filament discharges are used for basic plasma physics research,[1-5] for thin film deposition and etching,[6-8] and for ion sources for heating of fusion plasmas.[9,10] They are often used with a multidipole magnetic field to enhance the plasma density, quiescence, and uniformity.[1] Usually, the electron density and temperature are $n_e \approx 10^{15}$ m^{-3} and $T_e \approx 1$ eV.

Ion temperatures of typically[1] $T_i \approx 0.5$ eV have been measured with gridded electrostatic energy analyzers. In the literature, these ion temperatures have been called "anomalously" high.[11]

Several explanations for the anomalously high T_i have been suggested. First, Jones[12] proposed Langmuir's free-fall model as an explanation. The free-fall model relies on the inhomogeneity of the electric potential in the plasma. Ions are born nearly at rest throughout the discharge, and they fall down the potential hill. At a given point in the plasma, ions will have a distribution of energies because they were born throughout the plasma at various electric potentials. The resulting ion energy distribution may happen to be nearly Maxwellian.[4,12] D'Angelo and Alport[4] experimentally investigated the free-fall model and found that it only partially explains the anomalously high temperatures. To explain the high temperatures measured at the peak of the plasma potential hill, they suggested a second heating mechanism, "ion recycling." In the recycling model, the ions gain energy in the plasma sheaths, strike the vacuum vessel walls, and are reflected as energetic neutrals. These neutrals are subsequently ionized, producing a fast ion population. Third, Limpaecher and MacKenzie[1] and D'Angelo and Alport[4] questioned the resolution of their ion energy analyzers.

A considerable body of research[4,13-16] has shown that gridded energy analyzers have a temperature resolution on the order of several tenths of an electron-volt. This means that they are likely to be useless in measuring low ion temperatures, colder than 0.5 eV. Typically, electrostatic energy analyzers[13] consist of three parts: an entrance grid, a discriminating grid, and collector plate. The separations between these three parts have a profound effect on the energy resolution of the apparatus, as shown by the modeling of Donoso and Martin.[16] They found that the measured temperature has a significant error, and that this error varies with not only the separations between the parts, but also the structure of the grid fabric. The influence of the grid fabric on the measurement error is revealed in the experimental results reported by D'Angelo and Alport.[4] In two identical tests, they measured the ion temperature in a filament discharge, using a detector with tungsten grids. First they used a 40 lines/cm mesh and found that $T_i = 0.56$ eV, and then they used a 70 lines/cm mesh and found that $T_i = 0.28$ eV.

The values $T_i \approx 0.2$–0.5 eV that have been reported are suspicious simply because they are comparable to the energy resolution of the gridded analyzers. Clearly, an ion diagnostic with a better energy resolution is needed. For this paper, we used laser-induced fluorescence (LIF) to measure the temperature and density of the metastable excited-state ions. Our setup has a finer energy resolution than gridded energy analyzers, allowing the accurate measurement of temperatures as low as room temperature.

We found that the temperature of the metastable ions is $T_i^* = 0.028 \pm 0.007$ eV, which is close to room temperature, 0.025 eV. Using this data, we reexamine the controversy of "anomalous" ion temperatures in multidipole filament discharges. Additionally, we find that the metastable excited-state ion density is an accurate indicator of the ion density as a whole. This promises that LIF can find a good use in basic plasma physics, where spatially and temporally resolved density measurements are often needed.

II. APPARATUS

A. Multidipole device

A sketch of our plasma chamber is shown in Fig. 1. The vacuum vessel was divided into two sections, separated by a

[a] Present address: Engineering Research Center for Plasma Aided Manufacturing, Room 101, 1410 Johnson Drive, University of Wisconsin, Madison, Wisconsin 53706-1806.
[b] On temporary leave to: Max-Planck-Institut für Extraterrestrische Physik, 8046 Garching bei München, Germany.
[c] Present address: Department of Physics, West Virginia University, 209 Hodges Hall, Morgantown, West Virginia 26506-6023.

 0899-8221/91/102913-09$02.00

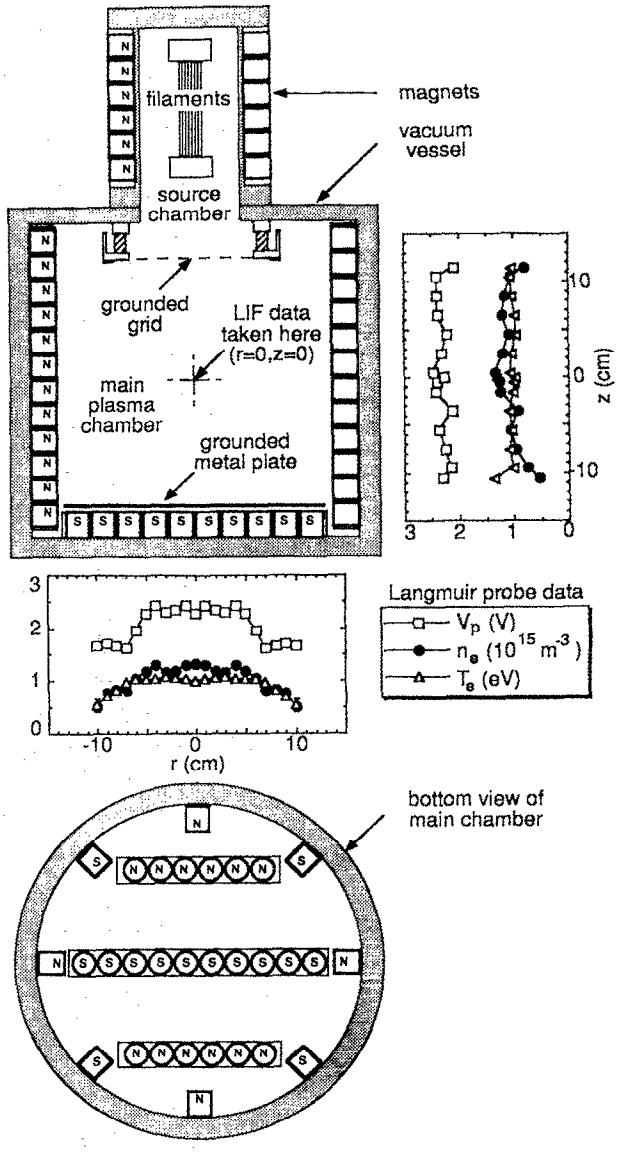

FIG. 1. Plasma chamber. Ceramic magnets are arranged in a line cusp geometry.[5] A grounded grid divides the device into a source chamber, containing the filaments, and a larger main chamber. The vacuum pump, gas inlet, water cooling on the source chamber, and ports are not shown. In the center of the main chamber, we used LIF to measure the metastable excited-state ion density n_i^* and temperature T_i^*. The axial (z) and radial (r) profiles of the plasma potential V_p, electron density n_e, and temperature T_e were obtained with a Langmuir probe. These profiles are for an argon plasma with a pressure $P = 0.050$ Pa, a discharge voltage $V_{dis} = 40.0$ V, and current $I_{dis} = 1.0$ A. For plasma processing, a substrate could be placed on the metal plate at the bottom of the chamber.

grid at ground potential. The filaments were housed in a source chamber with water-cooled stainless steel walls. Downstream there was a larger 32 cm diam main chamber where we characterized the discharge. It was made of black anodized aluminum to reduce scattered light, and it was fitted with Pyrex windows for making optical measurements.

Eight filaments were used, and they were made of thoriated tungsten, 12 cm long and 7 mil diam. To emit primary electrons, the filaments were heated by passing a current through them, and they were biased negatively at an electric potential we call the discharge voltage V_{dis}. The primary electrons sustain the discharge by ionizing neutral argon atoms. The heating voltage V_{heat} applied across the filaments can be varied to control the discharge current I_{dis} independently of the pressure P and V_{dis}. It is also important to note that the heating voltage results in the primary electrons having a range of energies, from eV_{dis} to $eV_{dis} + eV_{heat}$, depending on where along the length of the filament the electrons are emitted.

The multidipole magnetic field was provided by 19 rows of 2.5 cm long, 2.2 cm diam ceramic magnets, arranged in a line cusp geometry.[5] On the magnet surface, the field is 1.05 kG with a sample variation of $\pm$ 0.19 kG. Because the magnets are arranged in rows of alternating polarity, the field quickly diminishes away from the magnet surface. In the center of the main chamber, the magnetic field was measured to be less than 7 G. Inside the main chamber, the magnets are covered with 1 mm thick stainless steel anodes that were grounded.

Langmuir probe data were taken in the center of the main chamber and at additional axial and radial positions. This data yields the profiles in Fig. 1 of the plasma potential V_p, electron density n_e, and temperature T_e.

B. LIF diagnostic

Using sub-Doppler LIF[17] we measured the time-averaged velocity distribution function of metastable excited-state ions $(Ar^+)^*$. This was done by firing a laser through the plasma and recording the intensity of the emitted fluorescence, as shown in Fig. 2. Only those ions with a velocity satisfying the Doppler shift condition,

$$2\pi\Delta\nu = \mathbf{v}\cdot\mathbf{k} = v_{\parallel}k, \tag{1}$$

were excited by the laser. Here $\mathbf{k}$ is the incident laser photon wave vector, $\mathbf{v}$ is the ion velocity, $v_{\parallel}$ is the component of the ion velocity parallel to the direction of the laser beam, and $\Delta\nu$ is the difference between the laser frequency and the transition frequency of a stationary ion. The spectral line shape can be measured by tuning the laser frequency through the line and recording the fluorescence intensity at each frequen-

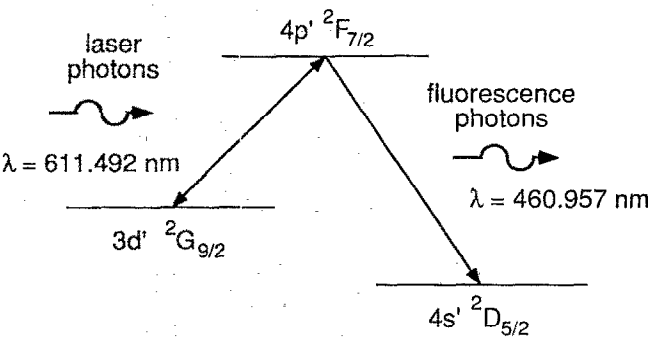

FIG. 2. Energy diagram of the laser-induced fluorescence process. For the experiment reported here, the argon ions are pumped from $3d'\ ^2G_{9/2}$ to $4p'\ ^2F_{7/2}$. Photons produced by spontaneous decay from $4p'\ ^2F_{7/2}$ to $4s'\ ^2D_{5/2}$ constitute the fluorescence signal. The shape of the spectral line is measured by scanning the laser frequency near the $3d'\ ^2G_{9/2}$-$4p'\ ^2F_{7/2}$ transition frequency and recording the fluorescence signal.

cy. This LIF line shape corresponds to the shape of the ion velocity distribution function. To be precise, one must recognize that the line shape is a function of only one of the three velocity components. Because of the vector dot product of $\mathbf{v}$ and $\mathbf{k}$, the LIF line shape corresponds to the shape of the velocity distribution $f_i^*(\mathbf{v})$, projected in velocity space along the direction of the laser beam, $v_\parallel$. We call this projection the reduced distribution function, $f_i^*(v_\parallel)$. The asterisk denotes the metastable excited state.

Careful attention was given to noise and other problems that can ruin the LIF measurements of $f_i^*(v_\parallel)$. We reduced noise levels in our experiment until random fluorescence from the plasma was the major remaining source. The blackbody emission noise was minimized by positioning the white-hot filaments out of the view of the detector, and by using black anodizing to absorb scattered light in the main chamber. To improve the signal-to-noise ratio further, we numerically averaged over 40 pulses at each wavelength of the laser. The distortions of $f_i^*(v_\parallel)$ from the natural linewidth,[18] pressure broadening,[19] Stark broadening,[19,20] Stark splitting,[21] Zeeman splitting,[21] and saturation broadening[22,23] were determined to be negligible.

The layout of the optical systems and the plasma is sketched in Fig. 3. We used a tunable dye laser (Lumonics HD-SLM), which was pulsed at 10 Hz, and operated in a single longitudinal mode[24] with a bandwidth of 400 MHz. This narrow bandwidth provided the fine velocity resolution we needed to measure ion temperatures as cold as room temperature. The laser beam passed through the center of the main chamber perpendicular to the axis of the discharge. To minimize saturation broadening, the intensity of the beam was reduced with neutral density optical filters. A telescope was used to expand the beam so that we did not burn up the filters. The telescope consisted of two 25 mm diam glass lenses, with focal lengths of -25 and $+75$ mm. A sample of the laser beam was diverted by a beam splitter through an iodine cell. We compared the iodine fluorescence spectrum to the spectrum tabulated[25] in an atlas in order to calibrate the laser wavelength.

The detection optics were positioned to view the plasma at an angle of 90° from the laser beam. A 150 mm focal length, 10 cm diam lens was used to focus the fluorescence from the plasma onto a 5 mm wide slit. This slit determined the chord viewed by the detection optics. The intersection of this chord and the laser beam defined the region of the plasma that was probed by the LIF apparatus. This volume was 0.5 cm long, 0.5 cm high, and 1 cm wide, thereby offering good spatial resolution. Directly behind the slit, a 0.51 nm bandpass interference filter was used to reduce extraneous light, especially the white-hot glow from the filaments. The fluorescence was detected by a photomultiplier tube (Thorn EMI 9659QB). We made no effort to calibrate the sensitivity of the detection optics.

The data acquisition scheme is also sketched in Fig. 3. The LIF signal from the plasma was amplified by 30 dB using a 300 MHz bandwidth amplifier (C-Cor 4375A). The LIF signals from the plasma and the iodine cell were measured with a pair of gated integrators (Stanford Research SR250). The triggering of the integrators was adjusted by viewing the signals and the gates on a digital oscilloscope (LeCroy 9400). The gate width for the plasma signal was set to 100 nsec which was narrow enough that photomultiplier tube (PMT) shot noise was insignificant yet wide enough to capture all of the signal. Although it is common to use the analog averaging feature of boxcar integrators, we avoided this because it sacrifices signal-to-noise ratio and it results in a skewed line shape. Instead, we numerically averaged the signal. To do this, the "last signal out" from the integrators

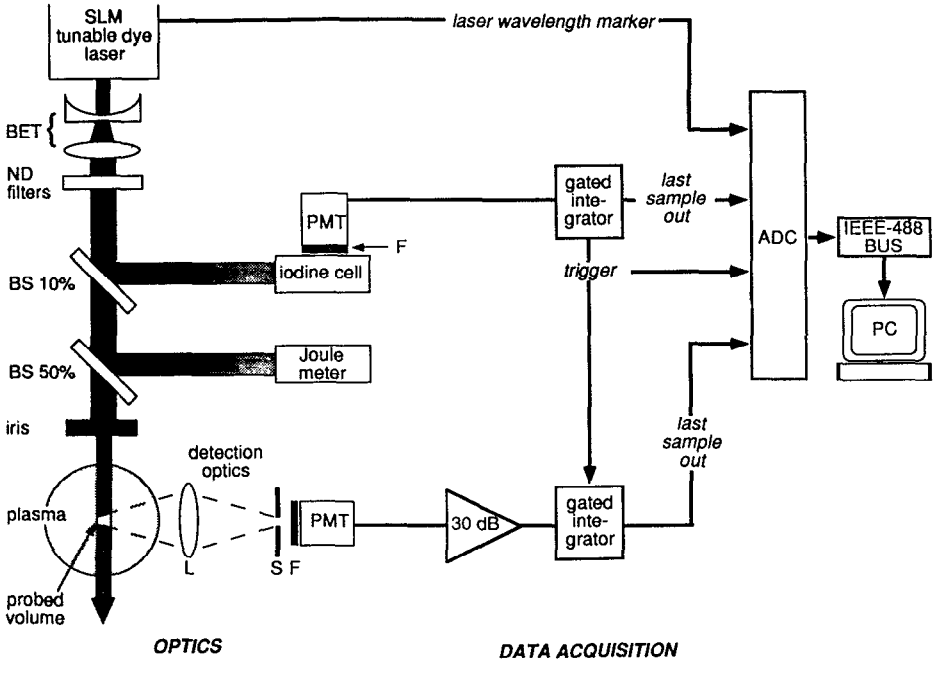

FIG. 3. Layout of the optical system and data acquisition for the LIF diagnostic. The optical equipment (not drawn to scale) includes a beam expanding telescope (BET), a set of removable neutral density (ND) filters, a movable adjustable iris, a 100 mm diam, 150 mm focal length lens (L), beam splitters (BS) of reflectivities 10% and 50%, a movable adjustable slit (S), two filters (F), and two photomultiplier tubes (PMT). We used an 0.51 nm bandpass interference filter for the plasma fluorescence and a red longpass filter for the iodine cell.

was digitized by an analog-to-digital converter (Stanford Research SR250), after each laser pulse. The signal was recorded on a computer and then averaged over 40 laser pulses, with each pulse equally weighted. All 40 pulses had the same single laser wavelength.

This procedure was repeated for 49 values of the laser wavelength to measure the line shape. The line shape was then numerically fitted to a Maxwellian. This yielded the metastable excited-state ion density, $n_i^* = \int f_i^*(v_\parallel)dv_\parallel$, and the metastable excited-state ion temperature, $T_i^* = (n_i^*)^{-1}\int M_i v_\parallel^2 f_i^*(v_\parallel)dv_\parallel$. The temperatures were corrected for the broadening resulting from the finite laser bandwidth.

III. RESULTS AND DISCUSSION

Using LIF and a Langmuir probe, we characterized the discharge in the center of the main chamber over a wide range of pressures, discharge voltages, and currents. We did not characterize the plasma in the source chamber because there were no windows to access that region. It would be difficult to measure there anyway, because the bright filament glow would be in a line of sight with the detection optics.

The LIF measurements of $f_i^*(v_\parallel)$ were made by tuning the laser through the 611.492 nm Ar^+ excitation line[26] of the $3d'\ ^2G_{9/2}$ metastable state,[27] and recording the intensity of the fluorescence[26] emitted at 460.957 nm.

One must ask whether all the ions, metastable and ground state, will have the same temperature and the same distribution function. The metastable ion state we probed in the experiment was only one of several in the plasma,[27,28] as listed in Table I. In an earlier experiment,[29] we measured $f_i^*(v_\parallel)$ for two different Ar^+ metastable states and confirmed that they had the same shape. While this test was done in a different type of discharge (a dc magnetron plasma), it lends confidence to the idea that all the metastable states will have the same ion temperature and similarly shaped $f_i^*(v_\parallel)$. There is also good reason to believe that the ground state ions had the same temperature and distribution function as the metastable states, as we argue in Appendix A. For these reasons, we believe our measurements are representative of the ions as a whole.

TABLE I. Metastable states of Ar^+. The energy levels listed are the thresholds for producing the metastable-state ions from ground-state neutral atoms by electron impact.[27] The authors of Ref. 36, using time-of-flight measurements, determined absolute lower limits for the lifetimes of the metastable ions. The actual lifetimes are likely to be much longer than the reported lower limit of 10 μsec.

Ground state	Metastable state	Threshold energy (eV)	Lifetime (μsec)	Ref.
$3p^5\ ^2P^0_{3/2}$		15.8		
	$3p^5\ ^2P^0_{1/2}$	16.0	18.9×10^6	28
	$3d\ ^4D_{7/2}$	32.2	>10	36
	$3d\ ^4F_{9/2}$	33.4	>10	36
	$3d\ ^4F_{7/2}$	33.5	>10	36
	$3d\ ^2F_{7/2}$	34.3	>10	36
	$3d'\ ^2G_{9/2}$	34.9	>10	36
	$3d'\ ^2G_{7/2}$	34.9	>10	36
	$3d'\ ^2F_{7/2}$	36.1	>10	36

A. Ion temperature

It was found that $T_i^* = 0.028 \pm 0.007$ eV, which is approximately room temperature, 0.025 eV. This result holds over the wide range of parameters we scanned, including the discharge current, discharge voltage, and pressure, as shown in Figs. 4–6. This finding, that the metastable ions are at room temperature, is the principal result of this paper.

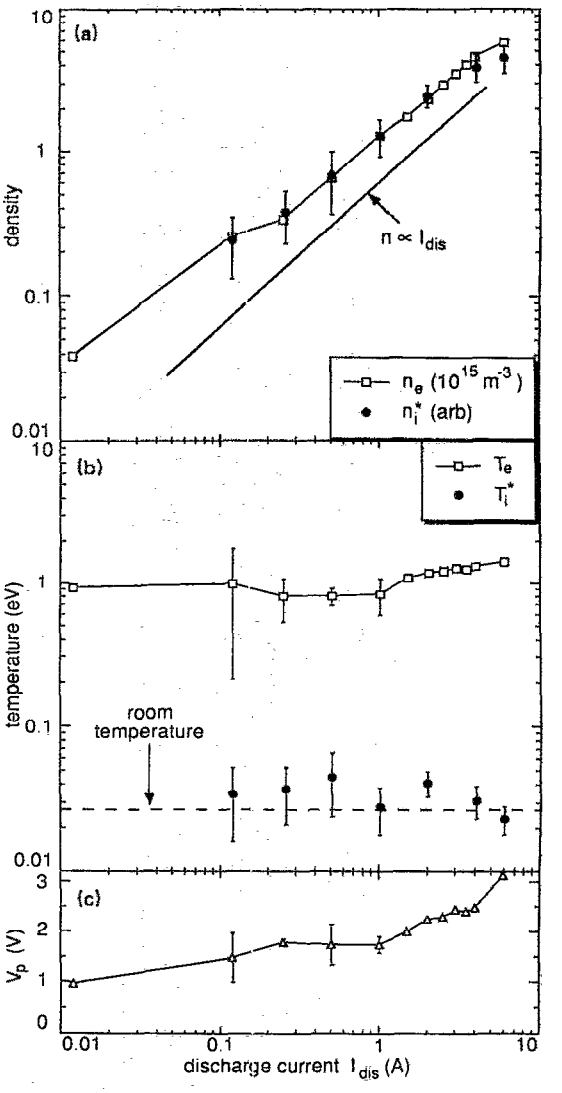

FIG. 4. Discharge current scan. Here $V_{dis} = 40$ V and $P = 0.050$ Pa were held constant. The ion temperature is close to room temperature. We also find that n_i^* is proportional to n_e and I_{dis}. Here, as in Figs. 5 and 6, the metastable ion density n_i^* is scaled so that its arbitrary units match the Langmuir probe measurement of n_e at $P = 0.050$ Pa, $V_{dis} = 40$ V, and $I_{dis} = 1.0$ A.

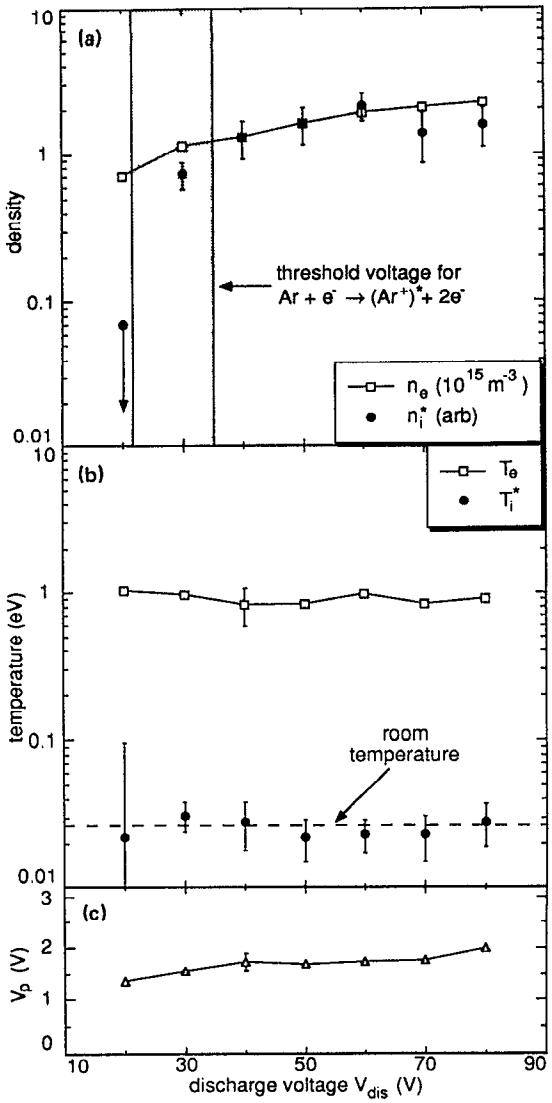

FIG. 5. Discharge voltage scan. Here $I_{dis} = 1.0$ A and $P = 0.050$ Pa were held constant. As in Fig. 4, we find that T_i^* is always near room temperature. Above the $V_{dis} = 34.9$ V threshold for the $Ar + e^-_{primary} \rightarrow (Ar^+)^* + 2e^-$ reaction, n_i^* is proportional to n_e. This scaling fails at $V_{dis} = 20$ V, which is below the threshold. There is a transitional region between these voltages, shown in gray, because of a potential drop along the filaments' length, $V_{heat} = 13.7$ V.

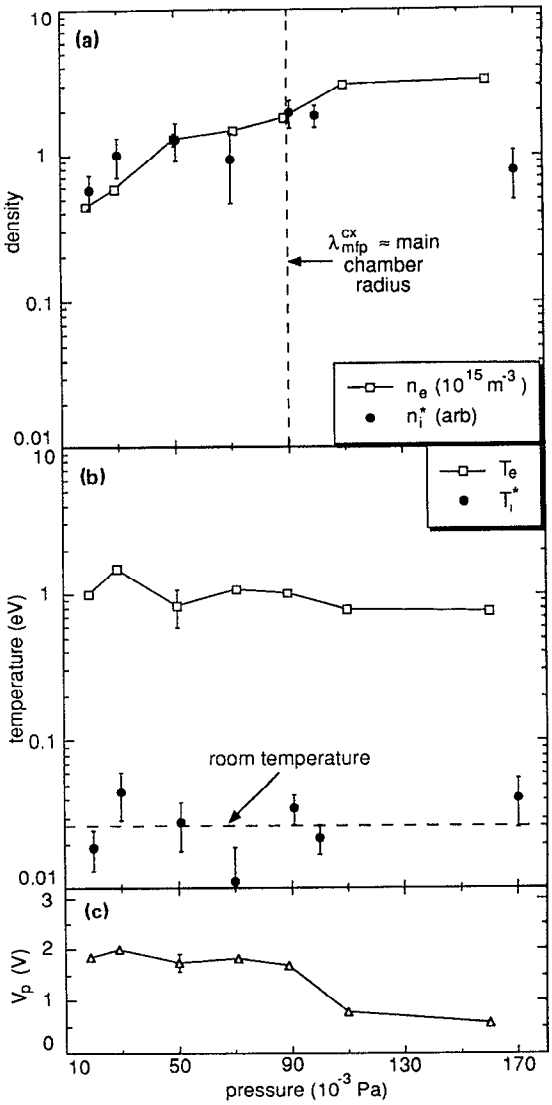

FIG. 6. Pressure scan. Here $I_{dis} = 1.0$ A and $V_{dis} = 40$ V were held constant. As in Figs. 4 and 5, we find that T_i^* is always near room temperature. At low pressure, where the mean-free path for inelastic collisions is long, n_i^* is proportional to n_e. Here, the mean-free path for inelastic collisions is approximated by the mean-free path for charge exchange[37] λ^{cx}_{mfp} of the ground-state ions, as explained in Appendix B. At high pressure, inelastic collisions depopulate the excited states of the ions.

B. Comparison to previous results

Our ion temperature stands in contrast to the values $0.2 < T_i < 0.5$ eV reported for multidipole filament discharges by energy analyzer users.[1,2,4] In Table II, we summarize our results and compare them to those of Refs. 1, 2, and 4. The lowest previously measured ion temperature known to us was reported by D'Angelo and Alport.[4] They measured the ion temperature with an energy analyzer and found that $T_i \approx 0.2$ eV. The discrepancy between their result and ours has several possible explanations, including differences in the detectors, the plasma sources, and the physics of heating ions. We discuss these explanations next.

Because of the different detectors that were employed, it is obvious to suggest that the discrepancy might be due to an inaccurate measurement. Gridded energy analyzers have been shown to have an energy resolution[4,13-16] that is on the order of several tenths of an electron-volt. Electrostatic analyzers are unsuited for measuring ion temperatures below this resolution. In comparison, we have demonstrated that sub-Doppler LIF can be used to resolve temperatures as low as room temperature, 0.025 eV. For this reason, we believe the temperatures measured using LIF are more accurate than those measured[1,2,4] with gridded energy analyzers.

Alternatively, the different configurations of the plasma source and vacuum vessels might account for the discrepancy in the measured temperatures. We used a tandem

TABLE II. Comparison to other argon multidipole filament experiments. Using LIF, we found that the ions are at room temperature. This stands in contrast to the "anomalously" high ion temperatures reported by researchers using gridded ion energy analyzers.[1,2,4]

	This paper	Limpaecher and MacKenzie[1]	Hershkowitz *et al.*[2]	D'Angelo and Alport[4]
Apparatus:				
Ion detector	LIF	analyzer	analyzer	analyzer
Vessel size (liter)	27	86	50	75
I_{dis} (A)	0.012–6	1–20	not reported	not reported
V_{dis} (V)	20–80	60	70	40
P (Pa)	0.020–0.150	7×10^{-4}–0.133	0.0133	0.053
Measurements:				
V_p (V)	1–3	(−7)–2	not reported	1
n_e ($\times10^{15}$ m^{-3})	0.1–6	7–1000	10–50	30
T_e (eV)	0.5–2	2–7	3	1.5–2
T_i (eV)	0.028 ± 0.007	>0.5	0.3	0.2

chamber separated by a grounded grid, while the authors of Refs. 1 and 4 used single chamber configurations, and the authors of Ref. 2 employed a tandem chamber separated by a magnetic field. Our chamber is smaller and our plasma was less dense. One might expect these different configurations to result in slightly different plasma parameters. Given the plasma configuration we had, we did scan the plasma parameters over a very wide range. The fact that our result was always the same suggests that the plasma configuration was not a likely cause of the discrepancy. Nevertheless, it is impossible to completely rule out the possibility.

Other explanations of the discrepancy center on the physics of ion heating. The first explanation predicts that ion temperatures should be lower at the peak of the plasma potential. Termed free fall, this process has been shown to influence the value of T_i measured in the experiments of D'Angelo and Alport.[4] The free-fall model works as follows. Ions are born throughout in the plasma at points of various electric potential. While they are originally born with the energy of the neutral gas, which might be at room temperature, they can gain energy by falling down a potential hill. Consider now an observer at a given point in the plasma. The ions passing by the observer originated at various places and at various potential energies. So their energies have been augmented by various amounts. This will broaden the energy distribution function that the observer measures there. Its shape may be nearly Maxwellian,[4,12] so that it is meaningful to characterize it by an ion temperature. In general, the augmentation of the ion temperature due to this process should be least at the top of a potential hill. The ions there cannot gain energy by falling down a potential hill. In our experiment, we took LIF data at the peak of the plasma potential in the main chamber, as shown in Fig. 1. Thus, according to the free-fall model, we measured T_i^* where it might be expected to be coldest. The trouble with ascribing this explanation to our temperature measurement is that D'Angelo and Alport[4] also made measurements at the peak of the plasma potential, and their electrostatic detector indicated that $T_i\approx0.2$ eV. So there is still a discrepancy.

A second physical process, put forth by D'Angelo and Alport[4] as the recycling model, suggests that the ions are heated by a plasma surface interaction. Ions gain energy in the plasma sheaths and then strike the vacuum vessel walls. They are reflected as neutral atoms with energies greater than the average energy of the background gas. Thus, each reflected neutral atom increases the average energy or temperature of the background gas. The effectiveness of this process depends, among other factors, on the discharge current. The flux of ions to the surfaces is proportional to I_{dis}. Hence, the flux of reflected neutral atoms is $\propto I_{dis}$, and so is the energy supplied to the background gas. Because the ions are born at the temperature of the background gas, a higher discharge current should result in hotter ions, according to the recycling model. The augmentation in ion temperature should increase with I_{dis}. This can be tested experimentally. We did not observe any change in T_i^* as I_{dis} was increased from 0.12 to 6 A. Thus it appears that ion recycling is not an important heating mechanism in our plasma, at least for the range of discharge currents we covered.

This test shows that the recycling hypothesis cannot explain the discrepancy. The reason for this conclusion is our finding that T_i^* is independent of I_{dis}. This finding is consistent with the results of Limpaecher and MacKenzie.[1] They used discharge currents from 1 to 20 A, and did not report any variation in T_i. Their data, however, was obtained using a gridded energy analyzer, and so they would not have been able to detect as small a temperature increase as we could with LIF. Our measurements appear to be the most sensitive indication that ion recycling does not measurably heat the ions in a filament multidipole discharge like ours.

Of all the possibilities discussed above, we can rule out all but two. The discrepancy in ion temperature is due to either the poor low-energy resolution of electrostatic analyzers or the different configuration of the chamber. The most probable explanation is the inaccuracy of the electrostatic analyzers. This means that the ions probably are indeed at room temperature. This result is important because it is contrary to the existing conventional wisdom.

C. Density scaling

It was found in this experiment that the metastable ion density n_i^* scales linearly with both n_e and I_{dis}. This was determined by scanning the discharge current from 0.012 to 6 A while holding the pressure $P = 0.050$ Pa and $V_{dis} = 40$ V constant. The results are shown in Fig. 4.

This linear scaling, $n_i^* \propto n_e$, reveals some interesting physics about the production of the metastable ions. It shows that they are produced mainly by single-step ionization of neutrals by electron impact,

$$Ar + e^-_{primary} \rightarrow (Ar^+)^* + 2e^- .$$

If they had been produced instead in two steps, an ionization

$$Ar + e^-_{primary} \rightarrow Ar^+ + 2e^-$$

followed by an excitation

$$Ar^+ + e^-_{primary} \rightarrow (Ar^+)^* + e^- ,$$

then one would expect a different scaling, $n_i^* \propto n_e^2$. These and other atomic processes[27,30-32] are quantified in Table III. The cross sections for single-step production of ground-state[33] and metastable-state[27] ions by electron–neutral collisions are shown in Fig. 7. When the filament bias is in the range $35\ V < V_{dis} < 80$ V approximately 3% of the ions are born in a metastable state.

The single-step production of $(Ar^+)^*$ can only occur when the electron impact energy is above a threshold. This threshold is revealed at low discharge voltages. As expected, we found that the linear scaling $n_i^* \propto n_e$ does not hold when V_{dis} is low. For Fig. 5, the discharge voltage was scanned from 20 to 80 V while keeping $P = 0.050$ Pa and $I_{dis} = 1.0$ A constant. While the metastable excited-state ions are plentiful when the primary-electron energy (eV_{dis}) is greater than the threshold for $Ar + e^-_{primary} \rightarrow (Ar^+)^* + 2e^-$, they are scarce when the energy is below it. A transitional region, due to a heater bias applied across the filaments, is also seen in Fig. 5.

TABLE III. Rate of production of metastable excited-state argon ions $(Ar^+)^*$. Here we enumerate the collisions that can produce metastable excited-state argon ions $(Ar^+)^*$ in a low-temperature discharge. The single-step process (1) has the fastest rate, 1×10^{18} m^{-3} sec^{-1}. In computing the rates, we assumed that the discharge current is 1 A, the primary electrons energy is 40 eV, the neutral density is 2.69×10^{18} m^{-3}, the ion density is 2.69×10^{15} m^{-3}, and the impact energies are characterized by $T_i \approx T_n \approx 0.05$ eV. The flux assumed for the soft x rays in (3) and (4) assumes that they carry away less than 1/1000 of the power supplied to the discharge.

	Process	Relative rate of $(Ar^+)^*$ production	Ref.
(1)	$Ar + e^-_{primary} \rightarrow (Ar^+)^* + 2e^-$	1	27
(2)	$Ar^+ + e^-_{primary} \rightarrow (Ar^+)^* + e^-$	10^{-2}	30
(3)	$Ar + h\nu \rightarrow (Ar^+)^* + e^-$	$< 10^{-4}$	31
(4)	$Ar^+ + h\nu \rightarrow (Ar^+)^*$	$< 10^{-4}$	32
(5)	$Ar^+ + Ar \rightarrow (Ar^+)^* + Ar$	0	27
(6)	$Ar^+ + Ar \rightarrow Ar + (Ar^+)^*$	0	27
(7)	$Ar^+ + Ar^+ \rightarrow (Ar^+)^* + Ar^+$	0	27
(8)	$Ar^+ + Ar^+ \rightarrow (Ar^+)^* + (Ar^+)^*$	0	27

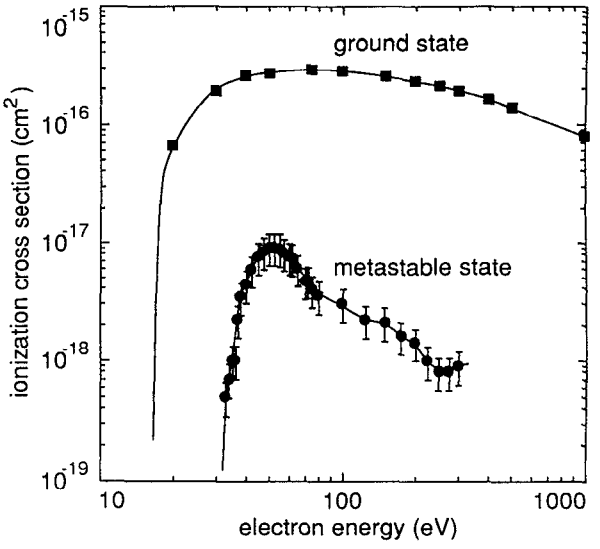

FIG. 7. Cross sections for electron-impact production of ground-state[23] and metastable-state[27] ions from ground-state argon atoms, as reported in the literature. The cross section for the metastable ions includes all of the metastable states except the $3p^5\,^2P^0_{1/2}$ state. In our experiment, the primary electrons had a range of energies, from eV_{dis} to $eV_{dis} + eV_{heat}$, where $V_{heat} \approx 14$ V and $20\ V \leqslant V_{dis} \leqslant 80$ V. For V_{dis} above 35 V, approximately 3% of the ions are produced in a metastable state.

The metastable ions in the experiment are usually lost from the discharge by striking a wall. This is not the case, however, at high pressures. The metastables are depopulated or quenched by inelastic collisions before they are strike a wall. As a result, the linear scaling $n_i^* \propto n_e$ fails to hold true. In our experiment, this occurred for pressures $P > 0.09$ Pa, as revealed in Fig. 6. The pressure was scanned from 0.020 to 0.170 Pa while holding $V_{dis} = 40$ V and $I_{dis} = 1.0$ A constant. Below 0.010 Pa the discharge extinguished. In Appendix B, we further discuss the quenching via inelastic collisions.

Our results above, revealing the range of parameters where the linear scaling $n_i^* \propto n_e$ applies, should be useful to other experimenters planning to use LIF to measure ion density. This is true whether the experimenters want to use sub-Doppler LIF, like ours, or broadband LIF. They may wish to operate their filament discharge with the pressure low enough so that the mean-free path between charge exchange collisions is longer than the machine size, and with the discharge voltage high enough for single-step production of metastables, $V_{dis} > 34.9$ V. These precautions will ensure that n_i^* serves as an accurate predictor of n_i.

IV. APPLICATIONS TO BASIC PLASMA EXPERIMENTS

In many basic plasma physics experiments, an antenna is used to excite a wave in the discharge. The wave may be launched continuously or in repeated pulses. The fluctuating ion density, electron density, or electric potential associated with the wave is recorded using a boxcar averager that is

synchronized to the oscillator for observing the temporal evolution of the wave. Experiments of this type have been carried out in many types of plasma confinement devices, including multidipole devices with filament sources.[34] Most often, electrostatic detectors are used: Langmuir probes (for measuring ion density or electron density), electrostatic energy analyzers, and electron beams (for measuring electric potential by means of the beam's deflection).

LIF has been used as a wave detector by Skiff and Anderegg.[35] Their experiment was performed in a long linear device with a uniform 2 kG magnetic field that confined an argon plasma. To observe the wave's temporal evolution, a pulsed laser was synchronized with the wave launcher. LIF provided a time-resolved measurement of the ion velocity distribution function. The success of their experiment relied on attaining an LIF signal strong enough to measure accurately the small fluctuations associated with the wave, which were typically 4% of the steady-state ion distribution function.

To our knowledge, no plasma wave experiments have been reported using LIF detection in a multidipole plasma. Our results lend encouragement to the idea of performing such measurements of the ion velocity distribution function in the unmagnetized center of a multidipole device. This would be useful for waves like the ion-acoustic mode and the ion-acoustic solitons, which require an unmagnetized plasma. When averaged over 40 pulses at each wavelength of the laser, our LIF signal-to-noise ratio was 5:1. Thus, one could have detected waves with a fluctuation amplitude of 20%. To observe waves with smaller fluctuations, one could average the signal over more laser pulses.

V. SUMMARY

Using the LIF diagnostic, we found that the ions are at room temperature in our multidipole filament discharge. This is in contrast to the "anomalously" high ion temperatures reported by researchers using gridded electrostatic energy analyzers. The experiments are comparable except that we measured only the metastable excited-state ions, and the vacuum vessels were not identical. Our findings suggest that the reports of higher temperatures are attributable to the poorer energy resolution of the energy analyzers.

In another result, we found that the metastable excited-state ion density scales linearly with both the discharge current and the electron density. This scaling breaks down if the mean-free path between inelastic collisions is short or the primary electron energy is less than the threshold for metastable ion production. These results suggest that in a discharge similar to ours, experimenters using LIF should operate with $V_{dis} > 35$ V and $P < 0.09$ Pa so that n_i^* serves as an accurate indicator of n_i.

ACKNOWLEDGMENTS

We wish to thank N. D'Angelo for a critical reading of this paper, and W. L. Weise and J. R. Fuhr for helping us locate the published lifetimes of $(Ar^+)^*$.

This work was funded by a grant from the Iowa Department of Economic Development.

APPENDIX A: METASTABLE VERSUS GROUND-STATE IONS

Here we examine the issue of whether the metastable ions that we measured should have the same temperature as all of the ions. The temperatures should be the same if the following three conditions are met.

First, the metastable and ground-state ions should be produced from the same population of neutral atoms. This is certainly the case in our discharge.

Second, the metastable and ground-state ions should be created at a uniform ratio throughout the discharge. This ratio of production rates can be expressed as

$$\frac{\nu_i(\mathbf{x})}{\nu_i^*(\mathbf{x})} = \frac{\int_{|\mathbf{v}|>v_t} \sigma_i(|\mathbf{v}|)|\mathbf{v}| f_e(\mathbf{x},|\mathbf{v}|)d|\mathbf{v}|}{\int_{|\mathbf{v}|>v_t} \sigma_i^*(|\mathbf{v}|)|\mathbf{v}| f_e(\mathbf{x},|\mathbf{v}|)d|\mathbf{v}|}, \quad \text{(A1)}$$

where $f_e(\mathbf{x},|\mathbf{v}|)$ is the electron speed distribution, v_t is the threshold speed for ion production, and σ_i and σ_i^* are the cross sections. To demonstrate that the ratio is uniform, we need to show that $f_e(\mathbf{x},|\mathbf{v}|>v_t)$ is independent of the position $\mathbf{x}$. Because the mean-free path for ionization in this discharge is long[33] (3.6 m at 0.04 Pa), and because there is little variation in V_p, the energy of the ionizing electrons should be approximately independent of position. Thus, the shape of $f_e(\mathbf{x},|\mathbf{v}|>v_t)$ probably depends only weakly on position, and the ratio in Eq. (A1) should be uniform.

Third, the lifetime of the metastable- and ground-state ions should be the same. A lifetime is determined by the loss mechanisms. For both the metastable and ground states, ions are lost mainly by escaping the plasma and not by atomic processes. Table I shows that the metastable state has a lifetime[36] of >10 μsec. This is longer than the ion transit time $\tau_{transit}$, which ranges from 1 to 7 μsec. Here, the ion transit time was calculated from

$$\tau_{transit} = \frac{e\int_{volume} n_e \, d\mathbf{x}}{I_{dis}},$$

where n_e is the electron density and e is the electron charge. Therefore, the metastables do not decay before they are lost. Thus ions of both states interact with the plasma for the same length of time.

For most parameters, these three criteria are satisfied in our discharge, and thus one should expect that $T_i^* = T_i$. An exception is at high pressures, $P > 0.09$ Pa, where inelastic collisions between ions and neutrals can depopulate the excited-state ions, and the third condition might not be satisfied.

APPENDIX B: COLLISIONAL QUENCHING OF METASTABLE IONS

Here we discuss the collisional quenching of metastable ions by inelastic collisions with neutrals. We argue that the mean-free path between inelastic collisions for metastable-state ions can be approximated by the mean-free path between charge exchange collisions,[37] λ_{mfp}^{cx}, for ground-state ions. This idea is useful in analyzing Fig. 6, which demonstrates collisional quenching at high neutral densities.

Using λ_{mfp}^{cx} as a measure of the mean-free path between inelastic collisions should reliably predict when collisional

quenching of the metastable ions becomes important. Inelastic collisions with the neutral gas can depopulate the metastable ions in the following ways:

$$(Ar^+)^* + Ar \rightarrow Ar^* + Ar^+, \quad \text{(B1)}$$

$$(Ar^+)^* + Ar \rightarrow Ar_{excited} + Ar^+ \rightarrow Ar + h\nu + Ar^+, \quad \text{(B2)}$$

$$(Ar^+)^* + Ar \rightarrow Ar^+ + h\nu + Ar, \quad \text{(B3)}$$

$$(Ar^+)^* + Ar \rightarrow Ar^+ + Ar^+ + e^-, \quad \text{(B4)}$$

$$(Ar^+)^* + Ar \rightarrow Ar^+ + Ar_{excited} \rightarrow Ar^+ + Ar + h\nu, \quad \text{(B5)}$$

$$(Ar^+)^* + Ar \rightarrow Ar + (Ar^+)_{excited} \rightarrow Ar + Ar^+ + h\nu. \quad \text{(B6)}$$

This is not an exhaustive list, but even so, we are aware of only cross section data for process (B1) and this data is only for ions with energy of 30 eV. So one cannot be sure of how to compute the mean-free path for collisional quenching.

One is encouraged, however, by the wealth of data on charge exchange collisions. The data[36] indicate that the mean-free path $\lambda^{\,l}_{mfp}$ for process (B1) is comparable to the mean-free path for charge exchange, $\lambda^{\,cx}_{mfp}$. The ratio $\lambda^{\,l}_{mfp}/\lambda^{\,cx}_{mfp}$ lies in the range 0.094–3.5. For this reason, we assume that the mean-free path between inelastic collisions for metastable-state ions can be approximated by the mean-free path between charge exchange collisions.

[1] R. Limpaecher and K. R. MacKenzie, Rev. Sci. Instrum. **44**, 726 (1973).
[2] N. Hershkowitz, K. N. Leung, and T. Romesser, Phys. Rev. Lett. **35**, 277 (1975).
[3] N. Hershkowitz, R. L. Goettsch, C. Chan, K. Hendricks, and R. T. Carpenter, J. Appl. Phys. **53**, 5330 (1982).
[4] N. D'Angelo and M. J. Alport, S. Afr. J. Phys. **5**, 81 (1982).
[5] K. N. Leung, T. K. Samec, and A. Lamm, Phys. Lett. A **51**, 490 (1975).
[6] H. R. Kaufman, J. J. Cuomo, and J. M. E. Harper, J. Vac. Sci. Technol. **21**, 725 (1982).
[7] T. E. Wicker and T. D. Mantei, J. Appl. Phys. **57**, 1638 (1985).
[8] Y. Ono, T Kurosawa, T. Sato, Y. Oka, and I. Hashimoto, J. Vac. Sci. Technol. A **4**, 788 (1986).
[9] K. N. Leung, in *The Physics and Technology of Ion Sources*, edited by I. G. Brown (Wiley–Interscience, New York, 1989), pp. 362–364.
[10] W. B. Kunkel, in *Fusion, Magnetic Confinement, Part B*, edited by E. Teller (Academic, New York, 1981), Vol. 1, pp. 137–139.
[11] N. D'Angelo and M. J. Alport, Plasma Phys. **24**, 1291 (1982).
[12] R. Jones, Plasma Phys. **20**, 717 (1978).
[13] C. P. DeNeef and A. J. Theiss, Rev. Sci. Instrum. **50**, 378 (1979).
[14] R. Jones, Rev. Sci. Instrum. **49**, 21 (1978).
[15] G. Donoso, P. Martin, and J. Puerta, Rev. Sci. Instrum. **57**, 1507 (1986).
[16] G. Donoso and P. Martin, Rev. Sci. Instrum. **57**, 1501 (1986).
[17] R. A. Stern and J. A. Johnson III, Phys. Rev. Lett. **34**, 1548 (1975).
[18] G. García and J. Campos, J. Quant. Spectrosc. Radiat. Transfer **34**, 85 (1985).
[19] H. R. Griem, *Spectral Line Broadening by Plasmas* (Academic, New York, 1974), p. 32.
[20] K. Miyamoto, *Plasma Physics for Nuclear Fusion* (MIT Press, Cambridge, MA, 1989), pp. 497–500.
[21] B. H. Bransden and C. J. Joachain, *Physics of Atoms and Molecules* (Longman, New York, 1983), p. 207, 229.
[22] M. J. Goeckner and J. Goree, J. Vac. Sci. Technol. A **7**, 977 (1989).
[23] M. J. Goeckner, J. Goree, and T. E. Sheridan, in *Proceedings of the Fourth International Laser Science Conference, Atlanta, 1988* (AIP, New York, 1989), pp. 761–766.
[24] M. G. Littman, Appl. Opt. **23**, 4465 (1984).
[25] S. Gerstenkorn and P. Luc, *Atlas du Spectre d'Absorption de la Molecule d'Iode*, (CNRS Editions, Paris, 1976).
[26] S. Bashkin and J. A. Stoner, Jr., *Atomic Energy Level and Grotrian Diagrams 2* (North-Holland, New York, 1978), pp. 192–229.
[27] P. Varga, W. Hofer, and H. Winter, J. Phys. B **14**, 1341 (1981).
[28] H. Nussbaumer and P. J. Story, Astron. Astrophys. **200**, L25 (1988).
[29] M. J. Goeckner, J. Goree, and T. E. Sheridan, J. Vac. Sci. Technol. A **8**, 3920 (1990).
[30] B. E. Cherrington, *Gaseous Electronics and Gas Lasers* (Pergamon, New York, 1979), p. 205.
[31] W. T. Silfvast, D. Y. Al-Salameh, and O. R. Wood II, Phys. Rev. A **34**, 5164 (1986).
[32] We have assumed that the cross section of this reaction is $\leqslant 1$ Å^2. This is 10^4 times larger than the cross section of reaction for $Ar^+ + h\nu \rightarrow (Ar^+)^* + e^-$, given in Ref. 31.
[33] F. J. deHeer, R. H. J. Jansen, and W. van der Kaay, J. Phys. B **12**, 979 (1979).
[34] E. K. Tsikis, S. Raychaudhuri, E. F. Gabl, and K. E. Lonngren, Plasma Phys. Controlled Fusion **27**, 419 (1985).
[35] F. Skiff and F. Anderegg, Phys. Rev. Lett. **59**, 896 (1987).
[36] K. Kadota and Y. Kaneko, Jpn. J. Appl. Phys. **13**, 1554 (1974).
[37] W. H. Cramer, J. Chem. Phys. **30**, 641 (1959).